

# H<sub>2</sub> production for MC fuel cell by steam reforming of ethanol over MgO supported Pd, Rh, Ni and Co catalysts

F. Frusteri<sup>a,\*</sup>, S. Freni<sup>a</sup>, L. Spadaro<sup>a</sup>, V. Chiodo<sup>a</sup>, G. Bonura<sup>a</sup>,  
S. Donato<sup>a</sup>, S. Cavallaro<sup>b</sup>

<sup>a</sup> *Istituto CNR-TAE, Via Salita S. Lucia Sopra Contesse 39, I-98126 Messina, Italy*

<sup>b</sup> *Dipartimento di Chimica Industriale e Ingegneria dei Materiali, Università di Messina, P.O. Box 29, S. Agata, I-98126 Messina, Italy*

Received 19 April 2004; accepted 27 July 2004

Available online 27 August 2004

## Abstract

The performance of MgO supported Pd, Rh, Ni and Co catalysts in the steam reforming of simulated bio-ethanol at MC fuel cell operative conditions ( $T = 650\text{ }^{\circ}\text{C}$ ) has been investigated. Rh/MgO shows the best performance both in terms of activity and stability, however, it seems not to be so selective towards H<sub>2</sub> production. Ni, Co and Pd catalysts are affected by deactivation mainly due to metal sintering. Ni/MgO displays the best performance in terms of H<sub>2</sub> selectivity (> 95%). A very low coke formation rate was observed on Rh/MgO catalyst, however, even on Ni/MgO catalyst coke formation occurs with modest rate. Kinetics measurements have shown that a significant difference in terms of metals specific activity exist: Rh sites resulted to be 2.2, 3.7 and 5.8 times more active than Pd, Co and Ni, respectively.

© 2004 Elsevier B.V. All rights reserved.

*Keywords:* Ethanol; H<sub>2</sub> production; MC fuel cell

## 1. Introduction

The growing need to reduce the environmental impact of the modern lifestyle imposes a continuous development of novel technologies aimed at a severe reduction of pollutant emissions, mainly from mobile sources, to ensure a tolerable quality of life in metropolitan areas. This has involved in the last years an extraordinary research effort for disclosing and synthesizing more effective and cleaner fuels. In perspective, the attainment of such goal would represent a milestone towards the exploitation of natural sources like biomass instead of oil as feedstock for fuels production. Different approaches have been attempted to convert biomass into a useful form of energy like pyrolysis, steam gasification. But also fermentation to obtain ethanol is very

attractive. Ethanol which is a clean burning fuel in use as oxygenated compound in reformulated gasoline (RFG) could be considered also as a suitable chemical storage system for H<sub>2</sub> production.

In the last years, the interest in the H<sub>2</sub> production from bio-ethanol has attracted a particular interest. Among different technologies proposed, attention was focused on the development of active, stable and selective catalyst for ethanol steam reforming reaction. At the moment metal sintering and coke formation seems to represent the main problems to overcome. Supported transition metal catalysts especially Co, Ni, Pt, Pd, Rh and Ru were investigated. Co based catalysts even though have been proposed as appropriate systems for steam reforming of ethanol [1] could be affected by deactivation mainly by sintering and surface Co oxidation [2]. Among noble metal based catalysts Rh is significantly more active and selective compared to Pt, Pd and Ru catalysts of similar metal loading [3,4].

\* Corresponding author. Tel.: +39 906 242 33; fax: +39 906 242 27.  
E-mail address: [francesco.frusteri@itae.cnr.it](mailto:francesco.frusteri@itae.cnr.it) (F. Frusteri).

Steam reforming of ethanol on Ni catalysts supported on  $\text{La}_2\text{O}_3$ ,  $\text{Al}_2\text{O}_3$ , YSZ and MgO was recently investigated [5]. The observed higher activity and stability of Ni/ $\text{La}_2\text{O}_3$  was attributed to the formation of lanthanum oxycarbonate species ( $\text{La}_2\text{O}_2\text{CO}_3$ ) which reacting with surface carbon deposited during reaction prevent the Ni deactivation. Ni–Cu bimetallic catalyst, recently proposed, looks interesting but coke formation drastically affects such systems [6].

Cu–Ni–K/ $\gamma\text{Al}_2\text{O}_3$  catalysts were proposed for ethanol gasification at low temperature: limitation due to diffusional resistance has been observed [7].

In this work a comparison of MgO supported Rh, Pd, Co and Ni based catalysts in the steam reforming of simulated bio-ethanol to produce hydrogen for MC fuel cell is reported. The result of the study was identification of active and stable catalytic system, characterized by high hydrogen productivity, adequate to the requirements for a compact hydrogen generator for MCFC technology.

## 2. Experimental

### 2.1. Catalysts

Catalysts were prepared by impregnation method (incipient wetness) using MgO Martin Marietta ( $120 \text{ m}^2 \text{ g}^{-1}$ ) as carrier. Before impregnation MgO was stabilized in steam atmosphere at  $700 \text{ }^\circ\text{C}$  for 12 h. Catalysts were dried at  $80 \text{ }^\circ\text{C}$  for 12 h and calcined at  $400 \text{ }^\circ\text{C}$  in air for 24 h.

21% Ni/MgO was prepared using a toluene solution of Ni acetate while 21% Co/MgO catalyst was prepared using absolute ethanol solution of Co nitrate. 3% Rh/MgO and 3% Pd/MgO catalysts were prepared using Rh and Pd acetyl–acetonate as precursors and toluene as solvent. All catalysts were dried at  $80 \text{ }^\circ\text{C}$  for 24 h and then air calcined at  $400 \text{ }^\circ\text{C}$  for 12 h. Catalyst samples were pressed at 400 bar, crushed and sieved, and the 40–70 mesh fraction was used for the catalytic measurements.

### 2.2. $\text{H}_2$ temperature-programmed desorption

$\text{H}_2$  temperature-programmed desorption (H-TPD) measurements in the range  $-80$  to  $500 \text{ }^\circ\text{C}$  were performed using Ar as carrier gas flowing at  $30 \text{ STP cm}^3 \text{ min}^{-1}$  and  $\beta = 20 \text{ }^\circ\text{C min}^{-1}$ . Before measurements, catalyst sample (0.04 g) was reduced for half-an hour in flowing  $\text{H}_2$  ( $25 \text{ STP cm}^3 \text{ min}^{-1}$ ) at  $600 \text{ }^\circ\text{C}$ . Thereafter, the sample was cooled in flowing  $\text{H}_2$  to room temperature, equilibrated for 15 min, and then further cooled to  $-80 \text{ }^\circ\text{C}$  in  $\text{H}_2$  for 5 min. Then the  $\text{H}_2$  was shut off and the sample was purged by the carrier stream until the stabilization of the baseline ( $\approx 10 \text{ min}$ ). The H-

TPD was monitored and quantified by a TC detector connected with a PC. Before and after every H-TPD run, a calibration test of peaks area was made by injecting in the carrier gas a known amount of  $\text{H}_2$ , the reproducibility being better than  $\pm 3\%$ . Assuming the chemisorption stoichiometry  $\text{H}_2:\text{Me}_{\text{surf}} = 1:2$ , metal dispersion ( $D$ ) was calculated from the following experimental ratio

$$D(\%) = V_{\text{H}_2}/V_{\text{O}_2} \times 100,$$

where  $V_{\text{H}_2}$  ( $\mu\text{mol g}_{\text{cat}}^{-1}$ ) is the amount of hydrogen uptake at  $500 \text{ }^\circ\text{C}$ , corresponding to the fraction ( $\alpha$ ) of zero, while the surface average Me particle size ( $d_s$ ) was derived from the equation suggested by Smith et al. [8] assuming a spherical shape of the metal particle:

$$d_s(\text{nm}) = n/D(\%),$$

where  $n$  is 114 for Rh and Pd and 101 for Co and Ni, respectively.

### 2.3. Transmission electron microscopy

The morphology and the Me particle size distribution (PDS) of the fresh and used catalysts were analysed by a PHILIPS CM12 Transmission Electron Microscope (TEM) provided with a high resolution camera. Catalysts were ultrasonically dispersed in isopropyl-alcohol and a drop of such dispersion was deposited over a thin carbon film supported on a standard copper grid. The metal particle size distribution (PSD) was obtained by considering at least ca. 500 particles for each catalyst sample, while the volume–area average Me particle size ( $d_s$ ) was calculated by the following normal statistical formula:  $d_s(\text{nm}) = \sum_i n_i d_i^3 / \sum_i n_i d_i^2$ .

### 2.4. CHNS elementary analysis

Carbon deposited during reaction was evaluated by using a CHNS – Carlo Erba elementary analyser instrument. Few mg of used catalyst were encapsulated and treated at high temperature in air.  $\text{CO}_2$  produced during oxidation process was analyzed by a high sensitivity TC detector.

The list of catalyst samples along with the relative Me loading,  $\text{H}_2$ -uptake, MSA and metal dispersion values is reported in Table 1.

### 2.5. Catalytic measurements

Experiments were performed at atmospheric pressure in a fixed-bed linear quartz micro-reactor (i.d. = 4 mm;  $H_{\text{bed}} = 1.0\text{--}2.0 \text{ cm}$ ).

0.010–0.060 g of catalyst (grain size: 40–70 mesh) diluted with 150–300 mg of same sized carborundum (SiC) were used for the catalytic tests. Prior to each run, catalysts were reduced in situ at  $T = 725 \text{ }^\circ\text{C}$  for 1 h

Table 1  
Temperature programmed desorption and H<sub>2</sub>-O<sub>2</sub> titration measurements

Catalyst	Metal loading (wt%)	H <sub>2</sub> -uptake (μmol/gcat)	MSA (m <sup>2</sup> <sub>Me/gcat</sub> )	Dispersion (%)	d (nm)
Rh/MgO	3	23.2	2.1	16.0	7.1
Pd/MgO	3	21.1	2.0	12.8	8.9
Ni/MgO	21	80.5	6.3	14.0	7.2
Co/MgO	21	96.8	7.6	15.6	6.5

under flowing hydrogen and then cooled down to reaction temperature. Water/ethanol mixture was fed by isocratic HP 1100 pump and vaporized at 120 °C in a flow of N<sub>2</sub>. Experiments were performed at 650 °C, gas hourly space velocities (GHSV) ranging from 5000 to 300,000 ml<sub>EtOH</sub> h<sup>-1</sup> ml<sub>cat</sub><sup>-1</sup> and steam to carbon ratio (mol/mol) 4.2. The total flow corresponding at GHSV of 40,000 h<sup>-1</sup> was 124 ml/min (24 vol% N<sub>2</sub> – 68 vol% H<sub>2</sub>O – 8 vol% EtOH).

Reaction stream was analyzed “on line” by a Hewlett Packard gas-chromatograph model 6890 Plus, equipped with a three columns (Molecular Sieve 5 Å, Porapack Q and Hysep) system and a thermal conductivity detector (TCD). Nitrogen was used as internal standard to carefully evaluate the carbon balance. GC data were acquired and elaborated by HP-IB interfaced computer system (HP Chemstation).

### 3. Results and discussion

Typical results showing the ethanol conversion vs. reaction time are presented in Fig. 1. A significant difference among catalysts both in terms of initial activity and stability can be observed. Thus, Rh/MgO catalyst resulted to be the most active and stable system, on the contrary Co, Ni and Pd catalysts are affected by a significant initial deactivation. In particular, Pd/MgO drastically deactivates during the first 5 h of reaction, losing almost 75% of its initial activity.

The corresponding product distribution shown in Fig. 2 reveals a similar behaviour for Rh, Co and Ni based catalysts which is characterised by a high CO<sub>2</sub>

selectivity (about 70%). However, it is interesting to note that Rh, which is the most active system, give rise to the formation of significant amount of CH<sub>4</sub> (10%). The behaviour of Pd/MgO catalyst was different. On the contrary of what observed on Rh, Co and Ni catalysts, the product distribution changes as the reaction proceeds. In particular, as the catalyst deactivates (see Fig. 1) the CO<sub>2</sub> selectivity significantly decreases (from 32% to 12%) in concomitance with a progressive increasing of CO selectivity (from 31% to 50%). Ethylene and acetaldehyde are both present in traces at the beginning of reaction but as the catalyst deactivates their concentration significantly increase reaching 6% and 15%, respectively.

In contrast with the active scale deducible from the results shown in Fig. 1 (Rh > Co > Ni > Pd) Ni/MgO catalyst resulted to be the most selective system toward hydrogen production. Selectivity values higher than 95% were obtained on such catalyst while on Co, Rh and Pd catalysts H<sub>2</sub> selectivity (see Fig. 3) never exceeded 92% (91%, 92% and 75%, respectively).

The difference observed in terms of product distribution could be explained on the basis of the reaction mechanism which, according also to our results recently published [9], can be presented by the scheme shown in Fig. 4. Ethanol is firstly dehydrogenated to acetaldehyde which subsequently decomposes into CH<sub>4</sub> and CO. These last ones by steam reforming and water gas shift reactions give rise to the formation of H<sub>2</sub> and CO<sub>2</sub>. In conclusion this means that the composition of outlet stream would be controlled by methane SR and WGS reactions.

Coming back to the product distribution shown in Fig. 2 the behaviour of each catalyst could be explained considering its activity towards specific reactions involved in the reaction mechanism. For example, Rh is very active in acetaldehyde decomposition and WGS reactions but seems not to be so active in SR since CH<sub>4</sub> concentration remain high enough (> 10%) otherwise Rh could be also active in the CO<sub>x</sub> methanation, which is not considered in the reaction scheme. Co and Ni are very active in SR (low CH<sub>4</sub> concentration) but are not so active in acetaldehyde decomposition, while Pd shows a satisfying activity in acetaldehyde decomposition only.

Results obtained by operating at high space velocity (see Table 2) clearly show that a significant difference

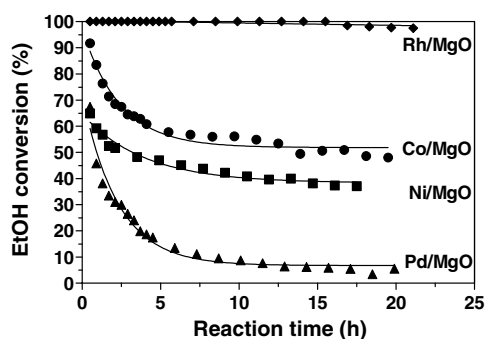


Fig. 1. Ethanol conversion as a function of time on stream:  $T = 650$  °C, GHSV = 40,000 h<sup>-1</sup>.

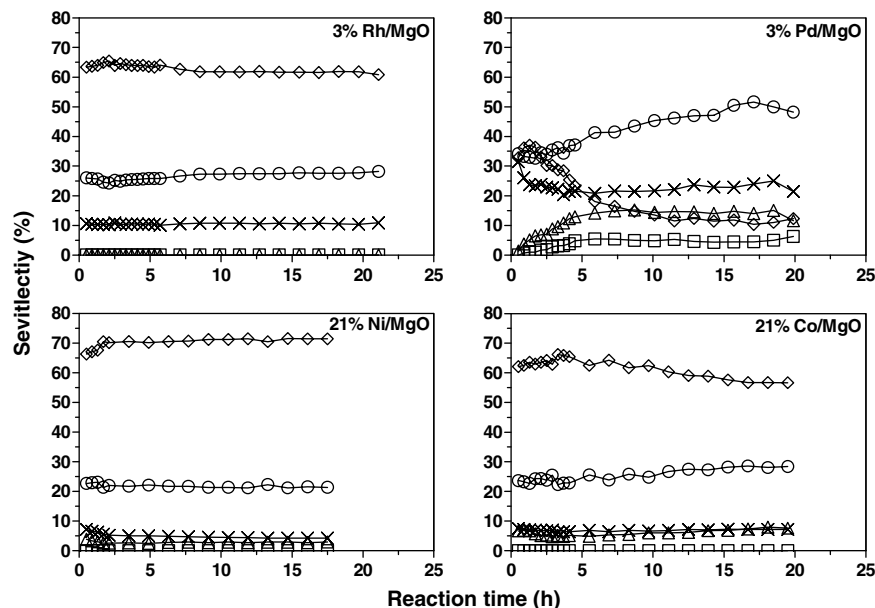


Fig. 2. Product distribution vs. time on stream:  $T = 650\text{ }^{\circ}\text{C}$ ,  $\text{GHSV} = 40,000\text{ h}^{-1}$  ( $\blacklozenge$ )  $\text{CO}_2$ , ( $\circ$ )  $\text{CO}$ , ( $\times$ )  $\text{CH}_4$ , ( $\triangle$ )  $\text{CH}_3\text{CHO}$ , ( $\square$ )  $\text{C}_2\text{H}_4$ .

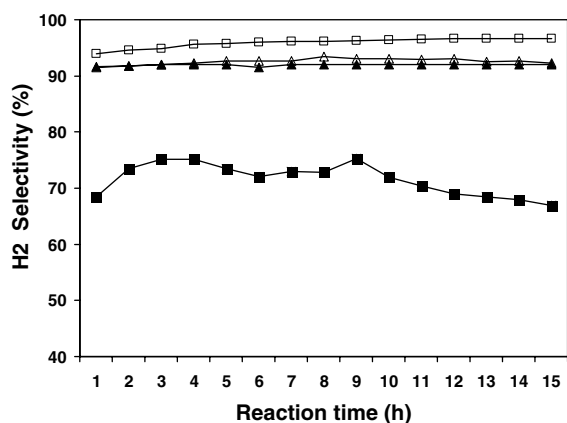


Fig. 3.  $\text{H}_2$  selectivity vs. time on stream:  $T = 650\text{ }^{\circ}\text{C}$ ,  $\text{GHSV} = 40,000\text{ h}^{-1}$  ( $\blacktriangle$ )  $\text{Rh/MgO}$ , ( $\triangle$ )  $\text{Co/MgO}$ , ( $\square$ )  $\text{Ni/MgO}$ , ( $\blacksquare$ )  $\text{Pd/MgO}$ .

among catalysts, both in terms of specific activity (TOF) and product distribution exists. Rh possesses a specific activity almost 4–6 times higher than that of Co and Ni, respectively and about double respect to Pd catalyst.

TEM analysis of fresh and used catalysts (see Fig. 5) revealed that Pd, Ni and Co are affected by metal sinter-

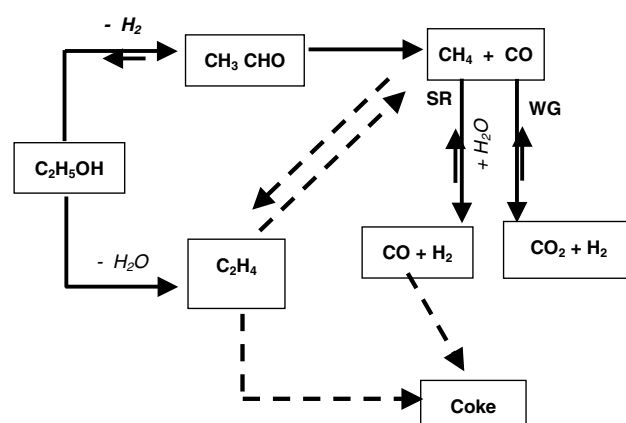


Fig. 4. Reaction mechanism scheme of ethanol steam reforming.

ing while Rh seems not to be influenced by a such problem since its mean particle size does not change significantly during reaction. By comparing results shown in Figs. 1 and 4 it can be concluded that a direct relationship exists between metal sintering and catalysts deactivation: the higher is the metal sintering the higher is the lost of catalytic activity.

Table 2

Steam reforming of ethanol: a comparison in terms of product distribution and TOF at high space velocity

Catalyst	EtOH conv (mol%)	Product distribution (vol%)					TOF ( $\text{s}^{-1}$ )
		$\text{CO}_2$	$\text{C}_2\text{H}_2$	$\text{CH}_3\text{CHO}$	$\text{CH}_4$	$\text{CO}$	
3% Rh/MgO	16.46	67.1	–	5.3	8.1	19.5	12.1
3% Pd/MgO	6.79	32.8	–	14.5	21.7	31.8	5.5
20% Co/MgO	19.00	44.4	–	31.2	5.6	18.8	3.3
20% Ni/MgO	10.36	58.2	–	19.6	5.7	16.5	2.1

$\text{GHSV} = 300,000\text{ h}^{-1}$ .

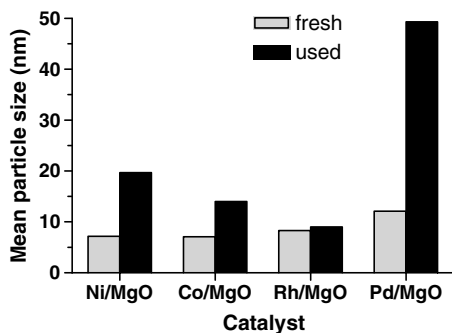


Fig. 5. Mean particle size of supported catalysts evaluated by TEM measurements:  $t = 20$  h;  $T = 50$  °C, GHSV = 40,000 h<sup>-1</sup>.

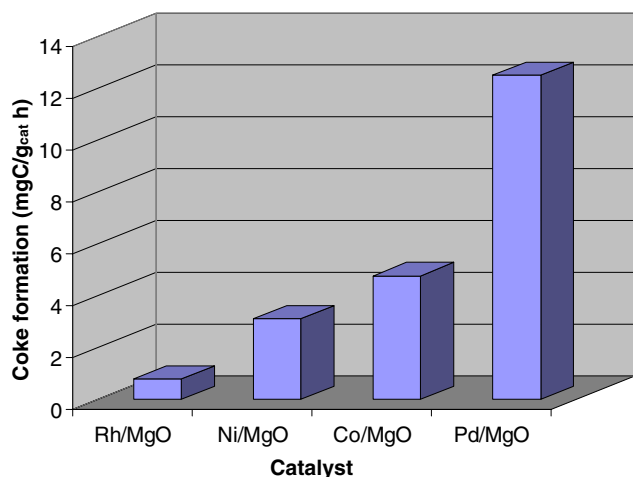


Fig. 6. Coke formation evaluated by CHNS elementary analysis of used catalysts: tests performed at GHSV = 40,000 h<sup>-1</sup>,  $T_R = 650$  °C for 20 h of reaction.

Another important factor to be taken into account in ethanol steam reforming at high temperature is the coke formation. As it is well known, the hydrocarbon reforming reactions are usually affected by coke formation which depends upon the reaction conditions and the physico-chemical properties of both catalyst and hydrocarbon. In our specific case, the high reaction temperature used ( $T = 650$  °C) and the low thermal stability of ethanol, represent the main serious problems for coke formation.

To compare the performance of catalysts in terms of coke formation, samples used at 40,000 h<sup>-1</sup> for 20 h were analyzed by CHNS. Results shown in Fig. 6, clearly indicate that coke formation occurs on Pd/MgO catalyst with higher rates than that observed on Rh, Ni and Co catalysts, respectively. The large amount of coke formed on Pd/MgO was probably caused by

activity of such catalyst in ethanol dehydration reaction with formation of ethylene (see Fig. 4) which is a known coke formation precursor. Coke formation is drastically inhibited on Rh/MgO catalyst, however, also on Ni/MgO and Co/MgO catalysts modest amount of coke were formed if compared with coke formation values reported for catalyst supported on acidic carrier ( $> 100$  mg/g<sub>cat</sub> h) [6]. Seems to be evident that the basic character of MgO would contribute to inhibits the formation of ethylene, in addition MgO could also modify the electronic properties of metal which, as previously vindicated, is a key both to inhibit the reactivity of Ni particles towards CO dissociation and to promotes a stronger interaction of Ni atoms with electron-acceptor O<sub>(ads)</sub> intermediates [10].

#### 4. Conclusions

H<sub>2</sub> can be efficiently produced by ethanol steam reforming on MgO supported metal catalysts. Rh/MgO shows the best performance both in terms of activity and stability, however, seems not to be so selective towards H<sub>2</sub> production. On the contrary Ni/MgO, even though it is affected by initial deactivation mainly due to the metal sintering, it is characterised by the highest H<sub>2</sub> selectivity ( $> 95\%$ ). Rh/MgO was the most resistant catalyst towards coke formation, however, also on Ni/MgO coke forms with very low rate, if compared with those vindicated by other authors on Ni supported on acidic carrier.

#### References

- [1] J. Llorca, N. Homs, J. Sales, Pilar R. de la Piscina, J. Catal. 209 (2002) 306–317.
- [2] S. Freni, S. Cavallaro, N. Mondello, L. Spadaro, F. Frusteri, Catal. Commun. 4 (2003) 259–268.
- [3] K. Liguras, D.I. Kondarides, X.E. Verykios, Appl. Catal. B 43 (2003) 345–354.
- [4] F. Auprêtre, C. Descorme, D. Duprez, Catal. Commun. 3 (2002) 263–267.
- [5] A.N. Fatsikostas, D.I. Kondarides, X.E. Verykios, Catal. Today 75 (2002) 145–155.
- [6] V. Klouz, V. Fierro, P. Denton, H. Katz, J.P. Lisse, S. Bouvot-Mauduit, C. Mirodatos, J. Power Sources 105 (2002) 26–34.
- [7] F. Mariño, M. Boveri, G. Baronetti, M. Laborde, Int. J. Hydrogen Energy 29 (2004) 67–71.
- [8] J.S. Smith, P.A. Thrower, M.A. Vannice, J. Catal. 68 (1981) 270.
- [9] S. Cavallaro, V. Chiodo, S. Freni, N. Mondello, F. Frusteri, Appl. Catal. A 249 (2003) 119–128.
- [10] F. Frusteri, L. Spadaro, F. Arena, A. Chuvilin, Carbon 40 (2002) 1063–1070.